

Article

Photocatalytic Removal of Microbiological Consortium and Organic Matter in Greywater

Nazmiye Cemre Birben *, Ceyda Senem Uyguner-Demirel and Miray Bekbolet

Institute of Environmental Sciences, Bogazici University, Bebek, Istanbul 34342, Turkey; uygunerc@boun.edu.tr (C.S.U.-D.); bekbolet@boun.edu.tr (M.B.)

* Correspondence: cemre.birben@boun.edu.tr; Tel.: +90-212-359-7145

Academic Editors: Giusy Lofrano, Dionysios (Dion) Demetriou Dionysiou, Polycarpus Falaras, Suresh C. Pillai, Adrián M.T. Silva and Xie Quan

Received: 15 April 2016; Accepted: 13 June 2016; Published: 22 June 2016

Abstract: This study aimed to investigate TiO₂ photocatalytic degradation of synthetically-prepared greywater samples with differing compositional contents of organic matter (OM), anion concentration, and microbiological consortium. Treatment efficiency was followed through removal of organic matter content in terms of dissolved organic carbon (DOC), specific spectroscopic parameters, and bacterial inactivation. Photocatalytic degradation kinetics were expressed by pseudo first-order kinetic modeling. The best DOC removal rates were attained for greywater samples containing OM with lower molecular size fractions. In addition, either enhancing or reducing the effect of common anions as radical scavengers were observed depending on the composition and concentration of variables in the greywater matrix. Moreover, possibility of a photocatalytic disinfection process was found to be of a bacteria type specific in OM-loaded synthetic greywater samples. Photocatalytic destruction of fecal streptococci required longer irradiation periods under all conditions. Bacterial removal rates were found to be in the order of total coliform > fecal coliform > fecal streptococci, for low organic load greywater, and fecal coliform > total coliform > fecal streptococci, for high organic load greywater.

Keywords: bacterial consortium; greywater; organic matter content; TiO₂ photocatalytic degradation

1. Introduction

Greywaters are defined as all polluted domestic wastewater coming from showers, hand washing basins, laundry facilities, kitchen sinks, and washing machines, excluding any discharge from toilets [1,2]. Depending on many different factors, e.g., inter-regional differences with regard to development, consumption, applications, *etc.*, greywater may constitute 50%–80% of the total domestic wastewater with varying compositions in terms of its physical, chemical, and microbiological properties [3,4]. Gulyas and co-workers analyzed separately-collected greywater which was biologically treated in a vertical intermittently-fed constructed wetland. With a non-purgeable total organic carbon (TOC) concentration of 6 mg·L⁻¹, the greywater sample was characterized by size exclusion chromatography with organic carbon detection and the following classes of organic compounds were detected: polysaccharides, humic substances, building blocks (subunits of humic substances) and, only to a very low extent, “amphiphilic and neutral organics”, which are mainly represented by low-molecular weight trace organics [5]. Based on the variety of constituents, greywater sources may be classified into different groups with respect to their organic matter (OM) loading and solid content, such as “low-load grey water” and “high-load grey water”.

Greywater treatment technologies may comprise a wide range of alternatives, from a simple filtration and disinfection process, to involvement of physical, chemical, and biological process alone or combined [6]. Although some of those treatment processes give satisfactory results for the treatment of greywater, they still have several limitations in terms of removing complex organic matter, bacterial

content, and other recalcitrant pollutants present in aqueous matrix [7]. At this point, advanced treatment technologies have gained an interest due to their several advantageous properties. As one of the advanced oxidation technologies, the photocatalytic oxidation process provides an innovative and effective way of non-selective oxidation leading to complete mineralization under the specified conditions [8–11]. The mechanism of the photocatalytic oxidation process is based on the production of highly-reactive hydroxyl radicals under ultraviolet (UV, $\lambda < 380$ nm) irradiation in the presence of a semiconductor photocatalyst (e.g., TiO_2). Non-selective oxidation of contaminants, simultaneous bactericidal impact [12–16], and chemical-free application are some of the advantages that make the photocatalytic oxidation process more favorable for water and wastewater treatment. Recent advances in research and application of heterogeneous photocatalysis have been well documented in the literature [17,18]. Considering the suitability and potential application of photocatalysis for the treatment of greywaters, studies have been mainly focused on the degradation of organic matter content in terms of TOC and/or DOC [5,19] and other components, such as ammonia/ammonium, surfactants, etc., present in real or synthetic greywater samples [20,21]. However, photocatalytic disinfection potential should also be taken into consideration when talking about greywater containing various types of microorganisms in significant concentrations. Referring to a literature survey on photocatalytic treatment of greywater, it was found that almost all studies emphasized removal of organic matter content rather than simultaneous removal of organic matter and bacteria [5,22]. Through the literature, only Sanchez and co-workers were the ones who checked both organic matter content and bacterial removal in greywater by TiO_2 photocatalysis and they concluded that complete removal of bacteria was achieved in hotel greywater. In order to fill the gap in the literature, this study aims to investigate the applicability of TiO_2 photocatalysis on greywater treatment by monitoring OM degradation and bacterial inactivation kinetics simultaneously in synthetically-prepared greywater samples.

2. Results

2.1. Characterization of the Prepared Greywater Samples

Characteristics of synthetic greywater samples L1–L3 and H1–H3 with respect to the compositional differences in organic matter contents, anion contents and microbiological consortium are presented in Table 1. All of the parameters were experimentally determined according to the procedures outlined in the methodology section. Based on UV-vis and fluorescence measurements, DOC-normalized specific parameters were also presented. Specific UV absorbance, SUVA_{254} ($\text{m}^{-1} \cdot \text{mg}^{-1} \cdot \text{L}$), is defined as $\text{UV}_{254}/\text{DOC}$ in which UV_{254} denotes UV absorbance at $\lambda = 254$ nm and specific fluorescence intensity, SFI_{syn} , is defined as $\text{FI}_{\text{syn}}/\text{DOC}$ of which FI_{syn} denotes fluorescence intensity at $\lambda_{\text{max}} = 470$ nm.

It should be emphasized that although molecular size profiles displayed similar distributions irrespective of initial DOC contents, the composition of the organic matrix would be different due to applied pre-oxidation step prior to the preparation of the samples H1–H3. It could be assumed that HA molecular size < 3 kDa could resemble surfactant contribution although all of the humic sub-fractions could display surfactant properties due to possible micelle formation capabilities [23].

SUVA_{254} values were in the range of 6.26–8.50 $\text{m}^{-1} \cdot \text{mg}^{-1} \cdot \text{L}$. As a specific UV-VIS parameter, $\text{SUVA}_{254} > 4$ indicates the presence of mainly hydrophobic and aromatic moieties, whereas for SUVA_{254} ratios in the range of 2–4, humic matrix are normally dominated with a mixture of hydrophobic and hydrophilic fractions. $\text{SUVA}_{254} < 2$ significantly represents hydrophilic properties [24]. Correspondingly, SUVA_{254} values expressed high aromatic and hydrophobic OM fractions for all of the greywater samples. Furthermore, the variations attained in FI_{syn} values expressed the presence of diverse fluorophores in greywater samples. SFI_{syn} displayed a range of 5.62–8.98. Contrary to the highest SUVA_{254} of L2, the lowest SFI_{syn} was attained in H3 greywater sample.

Table 1. Characteristics of greywater samples.

Greywater	DOC, mg·L ⁻¹	UV ₂₅₄ , m ⁻¹	FI _{syn}	SUVA ₂₅₄ m ⁻¹ ·mg ⁻¹ ·L	SFI _{syn}	Bacterial Content TC	CFU/100 mL × 10 ⁴ FC	FS
L1	6.72	56.38	60.6	8.39	8.95	-	-	-
L2	6.44	54.74	57.8	8.50	8.98	-	-	-
L3	6.80	42.60	48.96	6.26	7.20	5.4	3.1	1.6
H1	13.0	103.5	85.61	7.96	6.59	-	-	-
H2	12.9	102.6	81.55	7.95	6.32	-	-	-
H3	16.6	126.9	93.28	7.65	5.62	7.2	5.4	1.8
Anions, mg·L ⁻¹								
Greywater	F ⁻	Cl ⁻	Br ⁻	NO ₂ ⁻	NO ₃ ⁻	SO ₄ ²⁻	H ₂ PO ₄ ⁻ /HPO ₄ ²⁻	
L1, L3, H1, H3	0.0431	0.402	0.982	0.534	0.214	0.292	0.405	
L2, H2	0.341	3.621	9.56	6.36	2.14	2.08	3.95	

DOC contents of L1–L3 composing of 100 kDa fraction of HA expressed an average value of 6.65 mg·L⁻¹ as indicated. UV₂₅₄ of L3 sample was considerably lower than L1 and L2 due to the effect of filtration which was applied prior to UV-vis measurements. Since bacteria mixture was retained on the 0.45 µm membrane filter, an instantaneous adsorption onto the organic matrix could diminish the UV absorbance at λ = 254 nm. DOC contents of H1–H3 expressed an average value of 14.2 mg·L⁻¹ being composed of non-oxidized, as well as oxidized, fractions of 150 mg·L⁻¹ HA as mentioned in detail in previous sections. On the other hand, UV₂₅₄ of H3 grey water sample was slightly higher than UV₂₅₄ of H1 and H2 in accordance with the higher DOC content (16.6 mg·L⁻¹). Percent molecular size distribution profiles of low OM and high OM in terms of DOC and UV₂₅₄ were presented in Table 2.

Table 2. Percent molecular size distribution profiles of low OM and high OM in terms of DOC and UV₂₅₄.

Molecular Size Fractions	Low OM	High OM
DOC		
<100 kDa and >30 kDa	59%	41%
<30 kDa and >3 kDa	31%	49%
<3 kDa	10%	10%
UV ₂₅₄		
<100 kDa and >30 kDa	62%	43%
<30 kDa and >3 kDa	35%	51%
<3 kDa	3%	6%

Anion contents displayed almost ten-fold difference between two groups of greywater samples, as expected and verified by analyses (Table 1). Anion contents of greywaters, either real samples or synthetically-prepared samples, have been measured and presented in the literature. Greywater from 32 houses with 192 time-proportional samples were characterized in terms of chemical parameters by Hernández-Leal and colleagues [3]. It was concluded that anions of greywater samples were found to be in the following ranges of: 36–96.7 mg·L⁻¹ for Cl⁻, 0.01–7.95 mg·L⁻¹ for NO₃⁻, 0.03–6.98 mg·L⁻¹ for PO₄³⁻, and 0.10–21.10 mg·L⁻¹ for SO₄²⁻, indicating that working anion concentrations of this study could be regarded as the representative of anion content of greywaters.

Moreover, TC and FC contents were different from each other and FS contents could be considered as similar. L3 greywater sample contained TC: 5.4 × 10⁴ CFU/100 mL, FC: 3.1 × 10⁴ CFU/100 mL, and FS: 1.6 × 10⁴ CFU/100 mL whereas H3 greywater sample contained TC: 7.2 × 10⁴ CFU/100 mL, FC: 5.4 × 10⁴ CFU/100 mL, and almost similar FS: 1.8 × 10⁴ CFU/100 mL.

2.2. Degradation of Organic Matter: UV₂₅₄ and DOC Removal

Photocatalytic treatment of greywater samples was followed by irradiation time-dependent UV-vis spectroscopic measurements to express the significance of the UV₂₅₄ parameter. As a representative example, UV-vis spectroscopic profiles of all of the grey water samples prior to photocatalytic treatment and following photocatalytic treatment of 60 min were presented (Figure 1A,B).

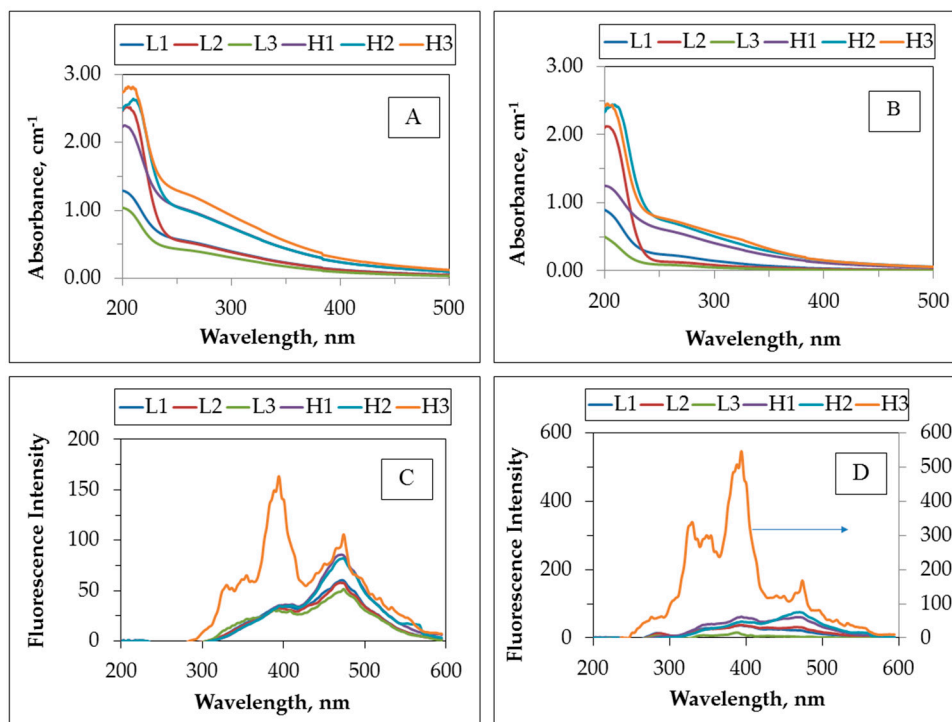


Figure 1. UV-vis absorbance spectra and synchronous scan spectra of greywater sample (A) UV-vis absorbance spectra of untreated greywater samples; (B) UV-vis absorbance spectra of photocatalytically-treated greywater samples; (C) synchronous scan spectra of untreated greywater samples; and (D) synchronous scan spectra of photocatalytically-treated greywater samples.

It could be visualized that UV-vis absorbance of all greywater samples followed a similar logarithmic decay profile of humic substances. Light absorption in the UV-vis region is a typical property of humic substances and several absorption wavelengths has been proposed for their spectroscopic characterization. Amongst them, UV absorbance at 254 nm was interchangeably measured with total organic carbon as a surrogate parameter to represent organic matter of humic substances [24,25]. Therefore, UV_{254} could be regarded as an effective parameter for the removal of UV-absorbing centers that were mostly aromatic in character. Moreover, Figure 1C,D showed the synchronous scan spectra of untreated greywater samples and photocatalytically-treated greywater samples, respectively. From a general perspective, all of the spectra displayed similar trends to the spectra attained for humic acids as expected [25]. Fluorescence intensities of the samples also illustrated a similar fashion, with the exception of H3, most probably due to the compositional variations leading to the formation of new fluorophoric groups at $\lambda_{emis} = 400$ nm (Figure 1C). Upon photocatalytic treatment, FI_{syn} decreased at $\lambda_{emis} = 475$ nm, however, H3 expressed the formation of new fluorophoric groups at around $\lambda_{emis} = 330$ nm that could be attributed to the release of organics through bacterial destruction.

Percent DOC removals under dark adsorptive conditions designated as $t = 0$ and removals following photocatalytic irradiation conditions at $t = 60$ min and $t = 90$ min were presented in Figure 2.

Regarding the definition of $t = 0$ condition at which the initial adsorption of the substrate was measured, the removals presented in Figure 2 simply indicated the surface of the photocatalyst was occupied by either OM or bacteria, or both, representing binary interactions. Low OM load greywater samples displayed a decreasing initial adsorptive removal trend ($t = 0$) with respect to the presence of anion contents (L1 vs. L2) and bacterial content (L1 and L2 vs. L3) (Figure 2). Contrary to these findings, in high OM load greywater samples variations in adsorptive DOC removals as 35.9%, 22.6%, and 37.1% for H1–H3 were observed, respectively. The presence of anions exerted an inhibitory effect

via electrostatic attraction to the positively charged TiO_2 surface in competition with the deprotonated centers of the OM. However, in the presence of bacterial consortium, adsorptive removal of OM could be enhanced by bacteria-OM interactions that could be successively removed by $0.45 \mu\text{m}$ filters prior to analysis. It should also be indicated that OM of H1–H3 samples were composed of oxidized humic fractions that could be considered as more hydrophilic in comparison to the L1–L3 samples. Moreover, upon 90 min of irradiation period, almost all of the greywater samples expressed DOC removal of $53\% \pm 4\%$. Due to the presence of low load OM as well as low anion content, the L1 greywater sample exhibited considerably higher DOC removal (70%), as expected. The removal trends displayed in Figure 2 could successfully be described by kinetics of photocatalytic oxidation as presented in Section 2.4.

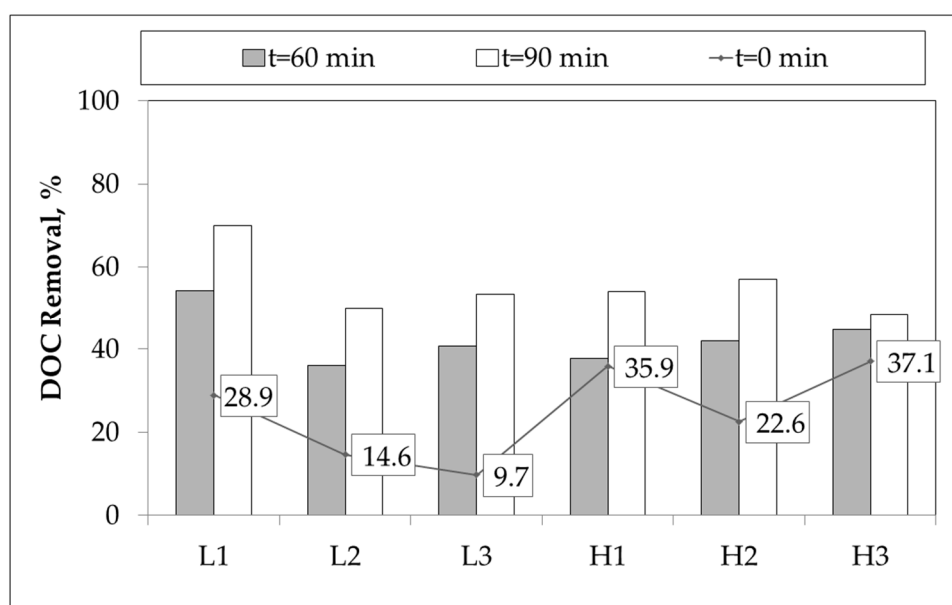


Figure 2. Irradiation time-dependent photocatalytic oxidation profiles of grey water samples in terms of DOC.

It could be inferred from Figure 2 that photocatalytic oxidation of low load greywater samples with lower OM content would give more effective results in terms of DOC removals displaying similarities with the study carried out by Sanchez and co-workers [21]. Considering the performance of the photocatalytic oxidation process, UV_{254} could be used as a surrogate parameter instead of DOC [24]. However, UV_{254} and DOC removal efficiencies of the greywater samples in 60 min were considerably different from each other (up to 80% removal of UV_{254} and less than 60% removal of DOC content). This could be attributed to adsorption and/or photocatalytic oxidation of the organic matter content of greywater samples having different UV absorptivity at $\lambda = 254 \text{ nm}$ [26]. Transformation of some of the organic fractions from unsaturated structure to saturated structure by photocatalytic oxidation process could be another possibility of different removal efficiencies of UV_{254} and DOC parameters [27].

Referring to the specific UV-vis parameter *i.e.*, SUVA_{254} , following photocatalytic irradiation of 60 min, the rest of L3 was composed of mostly hydrophilic OM, while L1 and L2 greywater samples were still composed of a mixture of hydrophobic and hydrophilic constituents (SUVA_{254} as 3.26 and 3.28, respectively). On the other hand, high-load greywater samples contained higher molecular size fractions with hydrophobic and aromatic moieties even after photocatalytic irradiation period of 60 min. Corresponding SUVA_{254} values were 7.46, 9.94, and 10.5 for H1–H3, respectively.

Following photocatalytic treatment, SFI_{syn} changes indicated the formation of new fluorophoric groups in H1–H3 greywater samples being significantly more pronounced in comparison to L1–L3

greywater samples. SFI_{syn} values were 7.64, 7.28 and 0.49 for L1–L3, respectively. Moreover, for high-OM load greywater samples SFI_{syn} were 7.45, 10.1 and 18.6 for H1–H3, respectively. SFI_{sync} was defined as DOC normalized synchronous fluorescence intensity at 470 nm (FI_{sync}). Although FI_{sync} values of H1 and H2 were decreased from 85.61 to 60.38 and from 81.55 to 75.08, the simultaneous decrease of DOC values from 13 to 8.1 for H1 and from 12.9 to 7.5 ended up with higher SFI_{sync} values.

It should be indicated that L3 and H3 samples also contained bacterial consortium subjected to photocatalysis upon which through cell destruction and following lysis, intracellular OM release should be expected. Therefore, contribution of the organic matrix formed through bacterial degradation would certainly affect the removal mechanism both UV_{254} and DOC.

2.3. Bacterial Inactivation

Bacterial inactivation via photocatalytic oxidation of greywater samples (L3 and H3) were presented in Figure 3. Although removal efficiencies after irradiation periods of 60 min and 90 min were given for simplicity purposes, kinetic evaluation were assessed by using whole range of irradiation periods. Following photocatalytic irradiation period of 90 min, almost complete destruction of TC and FC bacteria and 44% removal of FS bacteria were achieved for L3, whereas for the same photocatalytic irradiation period, H3 revealed removal efficiencies of 57%, 93%, and 6% for TC, FC, and FS, respectively.

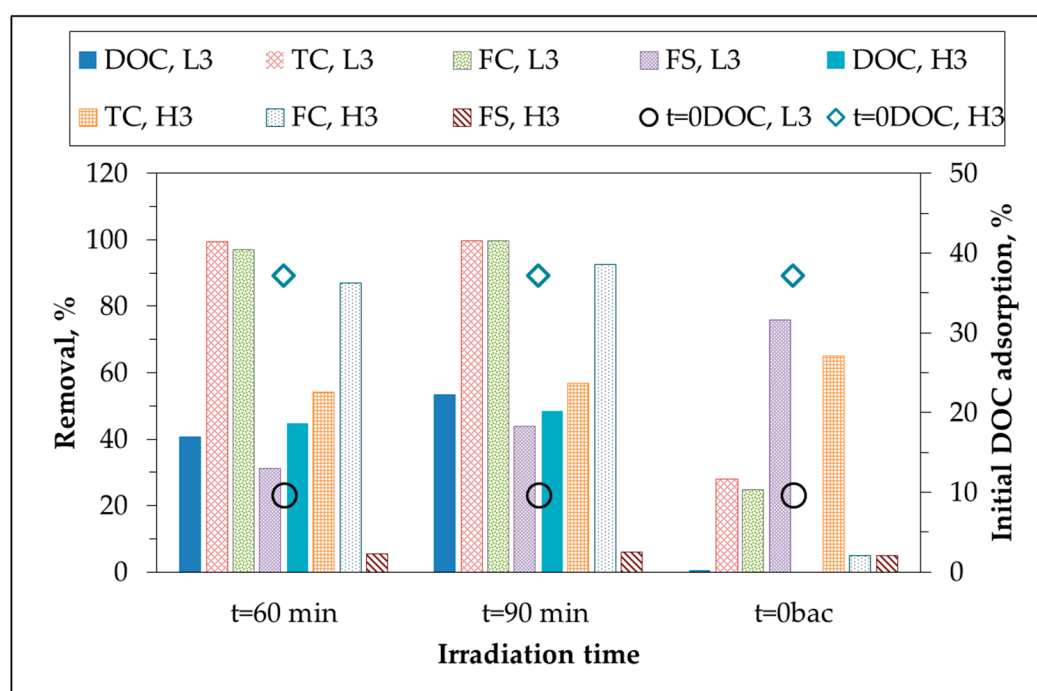


Figure 3. Photocatalytic bacterial removal profiles of greywater samples, L3 and H3; TC: total coliform; FC: fecal coliform; FS: fecal streptococci.

Initial adsorption mechanism is defined as the condition at which attachment of bacteria to the oxide surface upon an instantaneous introduction of TiO_2 and is one of the crucial steps prior to photocatalysis. Moreover, considering the larger size of bacteria in comparison to OM and anions, TiO_2 particles could possibly be adsorbed onto bacteria [28]. TiO_2 primary particle size was reported as 30 nm and dispersed particle size would be 200–215 nm in comparison to bacteria being greater than 0.45 μm [29]. As a consequence due to the low initial adsorption of TC bacteria (~25% for both L3 and H3), photocatalytic inactivation profiles of TC could be related to the Eley-Rideal mechanism rather than the surface-oriented Langmuir-Hinshelwood mechanism [30–32]. On the other hand, FC

inactivation profiles could be correlated to higher adsorptive removals (76% for L3 and 65% for H3). Initial adsorption of FS (5%) did not display any significant effect on the inactivation rate of H3 in 90 min of irradiation period contrary to the results attained for L3. Bacterial inactivation efficiencies of low-load greywater samples were found to be considerably higher than results revealed for high-load greywater samples which could be attributed to OM composition of high-load greywater samples constituting of high molecular weight organics.

2.4. Kinetic Considerations

Photocatalytic irradiation time-dependent degradation profiles revealed a basic logarithmic declining trend for both of the UV₂₅₄ and DOC parameters; thus, data were modeled by a pseudo first-order kinetic equation using the specified UV-vis parameter as well as DOC (Table 3). Pseudo first-order reaction rate (R) for the photocatalytic oxidation of low-load greywater with low anion content and bacteria (L3) was the most effective in terms of the removal of UV₂₅₄ parameter ($R = 1.33 \text{ m}^{-1} \cdot \text{min}^{-1}$). Although similar conditions existed for L3 and H3, with the exception of OM content, degradation rate of L3 was two times higher than that of H3. In a similar trend, photocatalytic degradation rate constants of L2 and H2 were noticeably different from each other. On the other hand, although their OM contents were different from each other (6.72 and 13.0 $\text{mg} \cdot \text{L}^{-1}$ respectively), UV₂₅₄ photocatalytic degradation rates of L1 and H1 expressed closer results indicating that the presence of specific anion concentration in the low range did not exert any significant effect in comparison to the effect of OM composition and content. Considering the dependence of kinetics and mechanism of oxidative degradation on the solution matrix, pseudo first-order degradation rates of UV₂₅₄ could be ordered as $L3 > L2 > H1 > H2 > L1 > H3$.

Table 3. Pseudo first-order kinetic model parameters of photocatalytically-treated greywater samples. k: pseudo first-order reaction rate constant; R: pseudo first-order reaction rate; and $t_{1/2}$: half-life.

Greywater	UV ₂₅₄			DOC		
	$k \times 10^{-2} \text{ min}^{-1}$	$R \text{ m}^{-1} \cdot \text{min}^{-1}$	$t_{1/2} \text{ min}$	$k \times 10^{-2} \text{ min}^{-1}$	$R \text{ mg} \cdot \text{L}^{-1} \cdot \text{min}^{-1}$	$t_{1/2} \text{ min}$
L1	1.29	0.727	54	1.21	0.0801	57
L2	2.18	1.19	32	0.724	0.0464	97
L3	3.12	1.33	22	0.833	0.0903	83
H1	0.853	0.880	82	0.741	0.0972	94
H2	0.791	0.811	88	0.852	0.110	81
H3	0.552	0.703	125	0.574	0.0752	122

The effect of solution matrix complexity on the pseudo-first order kinetic model parameters were observed and discussed by monitoring differences among different greywater samples in terms of removal of OM content expressed by DOC. DOC removal rates could be presented by the decreasing order of $H2 > H1 > L3 > L1 > H3 > L2$. In the presence of high load preoxidized OM, H1, and H2 greywater samples revealed comparatively higher DOC degradation rates. Although L3 sample contained bacteria, the presence of low-load OM and low-load of anions resulted in comparatively similar DOC removal rate. On the other hand, L1 and L2 samples exhibited lower DOC removal rates that could be explained by the composition of OM. Moreover, H3 sample expressed similar rate to L1 and L2 due to the presence of preoxidized OM, as well as bacteria.

Kinetic modeling of bacterial inactivation profiles of L3 and H3 greywater samples are presented in Figure 4A,B. Rapid inactivation of TC and FC bacteria in L3 were achieved even after a photocatalytic irradiation time of 20 min, reaching almost complete removal in 30 min of irradiation. However, in the case of H3, a comparatively slower inactivation rate was achieved for both TC and FC, indicating complete removal following a 120 min irradiation period. Contrary to these findings, the FS inactivation profile of L3 greywater sample displayed an induction period of 40 min during which only 20% FS was removed that could be attributed to a prevailing initial adsorption-desorption phase [31,33]. This phase was followed by rapid removal of 90% in 90 min. On the other hand, for the H3 greywater sample, this induction period was observed for 120 min followed by rapid inactivation phase reaching to almost

90% in 150 min. Pseudo first-order modeling of photocatalytic inactivation of bacteria in greywater samples was also assessed in Table 4.

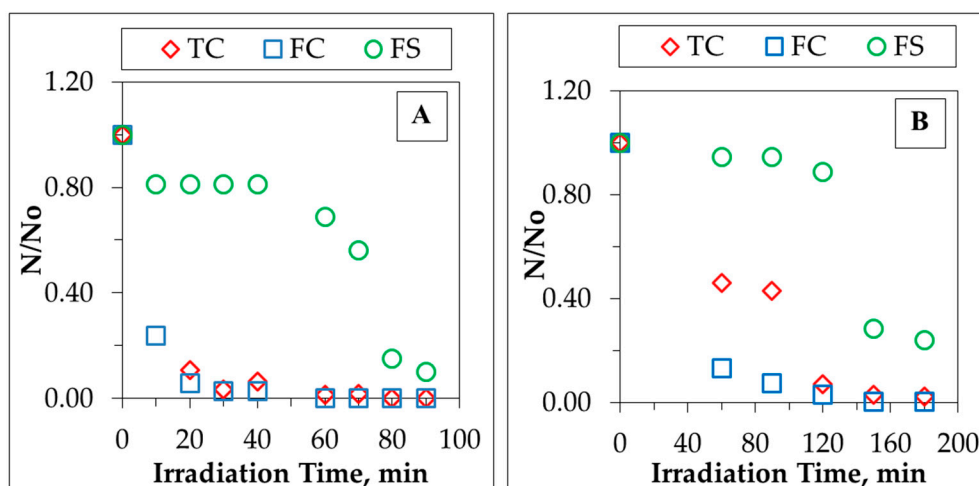


Figure 4. Normalized bacterial count profiles for L3 (A) and H3 (B) with respect to photocatalytic irradiation time.

Table 4. Photocatalytic bacterial inactivation kinetics of greywater samples.

Greywater	TC			FC			FS		
	$k \times 10^{-2}$ min^{-1}	R CFU100 $\text{mL}^{-1} \cdot \text{min}^{-1}$	$t_{1/2}$ min	$k \times 10^{-2}$ min^{-1}	R CFU100 $\text{mL}^{-1} \cdot \text{min}^{-1}$	$t_{1/2}$ min	$k \times 10^{-2}$ min^{-1}	R CFU100 $\text{mL}^{-1} \cdot \text{min}^{-1}$	$t_{1/2}$ min
L3	8.83	4.77×10^3	8	6.54	2.03×10^3	11	5.6	0.896×10^3	12
H3	2.26	1.63×10^3	31	3.23	1.74×10^3	21	0.8	0.14×10^3	87

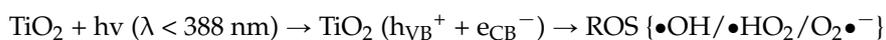
The observed differences could mainly be attributed to several reasons, such as (i) impact of organic carbon composition of greywater samples; (ii) differences in cell wall complexity and thickness between Gram positive (FS) and Gram negative bacteria such as coliforms (TC and FC); and (iii) the presence of common anions in solution matrix. Since the hydroxyl radical attack occurs on the cell wall of bacteria, attention should be paid to differences in cell wall complexity and thickness, which may be the reason of different photocatalytic inactivation profiles [34–36]. FS were known to be a sub-group of Gram-positive bacteria which have considerably thicker cell walls consisting of many complex layers of lipopolysaccharides and lipoproteins. On the other hand, referring to the sub-groups of Gram-negative bacteria, TC and FC bacteria have comparatively thinner cell walls composed of fewer layers of lipopolysaccharides and lipoproteins that could be less resistant to the photocatalytic oxidation process.

Acting as hydroxyl radical scavengers, common anions present in solution matrix could come up with a significant competitive reaction mechanism during photocatalytic degradation. In accordance with the previous findings presented in literature, the presence of common anions was expected to influence the photocatalytic degradation of organic matter, either due to direct effects via mechanistic pathway or indirect effects via alterations in the structure [37,38]. The induced outcome could be observed as inhibiting or enhancing factors [39]. Influence of sulfate and chloride ions on photocatalytic mineralization of humic acids have been studied by Bekbolet and co-workers revealing that the presence of both anions caused a significant reduction on degradation rate of humic acid [40].

Through the course of the photocatalytic treatment, prevailing interactions could be related to (i) pH dependent surface charge development and consecutive adsorptive interactions between components (TiO_2 -bacteria, TiO_2 -OM and TiO_2 -anions); (ii) interactions between solution matrix components: anion-bacteria, anion-OM, and bacteria-OM; (iii) light absorption leading to the formation of reactive oxygen species (ROS); and (iv) simultaneously occurring oxidation reactions between the reactive partners [31,41–43]. Based on these interactions, the reaction mechanism could be

presented in the simplified form as (OM_{ads} : organic matter adsorbed, OM_{ox} : organic matter oxidized, $(Bacteria)_{ads/free}$: bacteria either adsorbed or free in solution, and DOC_f : final dissolved organic carbon):

Primary reaction:



Organic matter content;

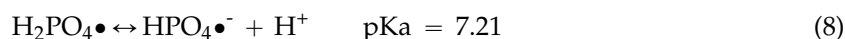
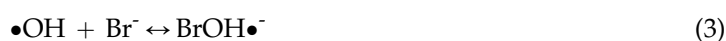


Bacterial consortium;



It should also be stated that the presence of varying amounts of organic fractions, as well as anions, could possibly interfere with the pH-dependent electrostatic interactions prevailing between the negatively charged bacterial species and partially negatively charged OM moieties due to the deprotonation of the carboxylic groups ($pK_a \sim 3-5$), anions, and the negatively/positively charged TiO_2 surface ($pH_{zpc} = 6.3$) [44,45]. Under neutral pH conditions, the surface of bacteria acquires a negative charge.

Inhibitory factors considered in the overall rate of the photocatalytic oxidation process could be attributed to the hydroxyl radical scavenging potential of the anions in the solution matrix as follows:



The observed scavenging effect was more pronounced overwhelming the slight enhancement that could be expected due to the formation of $SO_4\bullet^- / H_2PO_4\bullet$ radicals. Moreover, competitive oxidation reactions could also proceed between the anions and photogenerated h^+ on the surface of TiO_2 [41].

Despite the above presented effects due to the presence of anions, greywater samples could be successfully treated via photocatalysis achieving degradation of OM as well as inactivation of bacteria simultaneously.

3. Materials and Methods

3.1. Preparation of Synthetic Greywater Samples

Synthetic greywater samples were mainly composed of OM, anions, and bacteria. Based on the OM contents, two types of greywater samples were prepared, (i) low OM content ($DOC < 10 \text{ mg} \cdot \text{L}^{-1}$) and (ii) high OM content ($10 \text{ mg} \cdot \text{L}^{-1} < DOC < 20 \text{ mg} \cdot \text{L}^{-1}$). OM content was composed of humic acid (HA, Aldrich, St Louis, MO, USA, Na salt, Aldrich) and used as representative of organic matrix present in greywater samples. A working HA solution ($50 \text{ mg} \cdot \text{L}^{-1}$) was prepared by dilution of $1000 \text{ mg} \cdot \text{L}^{-1}$ stock solution and subjected to filtration through $0.45 \mu\text{m}$ filter followed by ultrafiltration through a 100 kDa molecular size membrane filter. A 100 kDa fraction of HA was further used for the preparation of low OM load greywater samples (L1–L3). Moreover, $150 \text{ mg} \cdot \text{L}^{-1}$ HA solution was subjected to partial oxidation via photocatalysis using $0.5 \text{ mg} \cdot \text{mL}^{-1}$ TiO_2 for an irradiation period of 60 min according to the method given by Bekbolet and colleagues [46]. Thus prepared HA

solution was comprised of organic fractions mostly oxidized and transformed into lower molecular size fractions. A mixture of OM was prepared by mixing an untreated 100 kDa fraction of HA and a photocatalytically-oxidized 100 kDa fraction of HA to form high OM load greywater (H1–H3). Humic acids are known to be surface active and can solubilize a wide variety of hydrophobic species due to a micelle-like organization in HA polymers in aqueous solution. Moreover, acting as amphiphilic species, humic acid's behavior in aqueous solution suggests that they form pseudomicelle aggregates analogous to the micelles from synthetic surfactant chemistry [23]. Therefore, representing both surfactant properties and multi component dissolved organic mixtures of real greywaters, untreated HA and photocatalytically-oxidized HA fractions were used as the components of synthetic greywater composition.

Mixed solutions of common anions were prepared in two different concentrations specified as “low anion content” and “high anion content” via appropriate dilution of the stock solution purchased from Dionex (product number: 0575909, Dionex Corporation, Sunnyvale, CA, USA). Anion mixture consisted of seven different common anions; F^- , Cl^- , Br^- , NO_2^- , NO_3^- , SO_4^{2-} , $H_2PO_4^-/HPO_4^{2-}$.

A mixed culture of bacteria as total coliforms (TC), fecal coliforms (FC), and fecal streptococci (FS) were selected as indicator organisms and were isolated from septic effluent in order to simulate fecally-transmitted microorganisms found in real greywater sources. Isolated bacteria were inoculated into appropriate cultures in order to attain an initial bacterial load of 10^4 CFU/100 mL⁻¹. Most of the literature studies on photocatalytic treatment of greywater focused on the removal of selected organic and/or inorganic compounds. However, a literature survey regarding the characteristics of greywater revealed that bacterial content of greywater could reach up to 10^5 – 10^7 CFU/100 mL⁻¹ [47,48] and should be considered as a problem due to their potential risk to health when considering greywater reuse for potable and non-potable purposes [49].

For simplicity purposes, the prepared synthetic greywater samples were described by using the abbreviations presented in Table 5.

Table 5. Abbreviations used for grey water samples.

Abbreviation	Grey Water Sample
L1	Low OM load grey water with low anion content
L2	Low OM load grey water with high anion content
L3	Low OM load grey water with low anion content and bacteria
H1	High OM load grey water with low anion content
H2	High OM load grey water with high anion content
H3	High OM load grey water with low anion content and bacteria

3.2. Experimental Setup and Procedure

50 mL of synthetic greywater sample (L1–L3 and H1–H3) from each stock solution (1 L) was used for photocatalytic oxidation experiments which were conducted in a completely mixed reactor utilizing UV-A light. A 125 W black light fluorescent lamp (BLF) emitting radiation between 300 and 420 nm with a maximum intensity at $\lambda_{max} = 365$ nm was used as the light source ($I_0 = 56$ W·m⁻²). Continuous stirring was provided by a magnetic stirrer. Detailed information about the experimental procedure was mentioned previously by Bekbolet and co-workers [46]. Evonik P-25 (Evonik Corporation, USA) with a photocatalyst loading of 0.25 mg·mL⁻¹ was used for both low load and high load greywater samples. Photocatalytic degradation experiments were performed for irradiation periods of 0–180 min with 10 min intervals. Moreover, $t = 0$ represented the initial condition upon which instantaneous adsorption of the components onto TiO₂ was assessed. All experiments were conducted under natural pH of the samples (pH~6–6.5).

3.3. Analytical Methods

All of the greywater samples were filtered through 0.45 μm membrane filters prior to analysis. Dissolved organic carbon (DOC, $\text{mg}\cdot\text{L}^{-1}$) measurements were performed by using Shimadzu TOC Vwp Total Organic Carbon Analyzer (Shimadzu Corporation, Kyoto, Japan). OM was characterized by absorbance measurements at $\lambda = 254\text{ nm}$ (UV_{254} , m^{-1}) using a Perkin Elmer Lambda 35 UV-vis double beam spectrophotometer with Hellma quartz cuvettes of 1 cm optical path length (Perkin Elmer Inc., Warrington, UK). Synchronous scan fluorescence spectra were acquired by a Perkin Elmer LS 55 Luminescence Spectrometer in the excitation wavelength range of 200–600 nm using the bandwidth of $\lambda = 18\text{ nm}$ between the excitation and emission monochromators (FI_{syn} , Perkin Elmer Inc., Warrington, UK). Anion concentrations were determined by ion chromatography (Dionex ICS-3000 ion chromatography, Dionex Corporation, Sunnyvale, CA, USA). Microbiological analyses of grey water samples were performed according to the membrane filter technique with reference to standard methods [50]. A pre-sterilized absorbent pad was placed into a Petri dish using a dispenser and 2 mL of culture media was pipetted onto the pad. Culture media containing the nutrients necessary for the growth of the specific target bacteria, such as total coliform (MF-Endo Broth, Merck Millipore Corporation, Bedford, MA, USA), fecal coliform (M-FC Broth, Merck Millipore Corporation, Bedford, MA, USA), and fecal streptococci (KF Agar, Merck Millipore Corporation, U.S.A.) was prepared particularly according to methodology given in standard methods. After a sterile membrane filter was centered on the filter support, the funnel top was attached and a well-shaken sample with a volume of 100 mL was filtered through the membrane followed by rinsing the sides of the funnel with 20–30 mL ultra-pure water. Then the membrane filter was removed from the filter base by sterile forceps and rolled onto the pad to avoid the formation of bubbles. Enumeration of bacterial cultures was done after Petri dishes were kept in the incubator at 37 °C for 22–24 h. A low power microscope with daylight was used to count colonies. Molecular size distribution profiles of the organic matrix was determined by using an Amicon 8050 (Amicon Corporation, Danvers, MA, USA) stirred cell ultrafiltration cell unit and membrane filters with nominal molecular size cutoffs as 100 kDa, 30 kDa, 10 kDa, and 3 kDa [51].

4. Conclusions

Considering the bacterial inactivation of L3 and H3, the most effective results for the removal of Total coliform (TC), fecal coliform (FC), and fecal streptococci (FS) were attained for L3 via photocatalytic oxidation. Photocatalytic destruction of FS required longer irradiation periods under all conditions indicating the influence of bacteria species irrespective of the greywater matrix. Bacterial removal rates were found to be in the order of $\text{TC} > \text{FC} > \text{FS}$ for L3 and in the order of $\text{FC} > \text{TC} > \text{FS}$ for H3. Moreover, the DOC removal rate constant observed for L3 was found to be higher than the DOC removal rate constant observed for H3. The reason could be attributed to the presence of an organic matrix rather than molecular size distribution profiles of organic matter. Special attention should be directed to the role of adsorptive interactions prevailing between organic components, bacterial consortium, and anions present in the aqueous media. Further research on the possibility of bacteria reactivation under favorable conditions, such as regrowth in the presence of organic and inorganic compounds originating from the lysis of the bacteria, is highly recommended.

Acknowledgments: Financial support provided by Research Fund of Bogazici University through project number 10480 is gratefully acknowledged.

Author Contributions: Ceyda Senem Uyguner-Demirel and Miray Bekbolet conceived and designed the experiments; Nazmiye Cemre Birben performed the experiments; Nazmiye Cemre Birben, Ceyda Senem Uyguner-Demirel and Miray Bekbolet analyzed the data; Nazmiye Cemre Birben, Ceyda Senem Uyguner-Demirel and Miray Bekbolet wrote the paper.

Conflicts of Interest: The authors declare no conflict of interest.

Abbreviations

The following abbreviations are used in this manuscript:

BLF	Black Light Fluorescent
CFU	Colony forming unit
DOC	Dissolved organic carbon
FC	Fecal Coliform
FS	Fecal Streptococci
H1	High organic matter load grey water with low anion content
H2	High organic matter load grey water with high anion content
H3	High load organic matter grey water with low anion content and bacteria
HA	Humic acid
L1	Low organic matter load grey water with low anion content
L2	Low organic matter load grey water with high anion content
L3	Low load organic matter grey water with low anion content and bacteria
OM	organic matter
ROS	Reactive oxygen species
TC	Total Coliform
TOC	Total organic carbon

References

- Eriksson, E.; Auffarth, K.; Henze, M.; Ledin, A. Characteristics of grey wastewater. *Urban Water* **2002**, *4*, 85–104. [[CrossRef](#)]
- Hourlier, F.; Masse, A.; Jaouen, P.; Lakel, A.; Gerente, C.; Faur, C.; Le Cloirec, P. Formulation of synthetic grey water as an evaluation tool for wastewater recycling technologies. *Environ. Technol.* **2010**, *31*, 215–223. [[CrossRef](#)] [[PubMed](#)]
- Hernández Leal, L.; Temmink, H.; Zeeman, G.; Buisman, C.J.N. Characterization and anaerobic biodegradability of grey water. *Desalination* **2011**, *270*, 111–115. [[CrossRef](#)]
- Friedler, E.; Hadari, M. Economic feasibility of on-site grey water reuse in multi-storey buildings. *Desalination* **2006**, *190*, 221–234. [[CrossRef](#)]
- Gulyas, H.; Choromanski, P.; Muellin, N.; Furmanska, M. Toward chemical-free reclamation of biologically pretreated greywater: Solar photocatalytic oxidation with powdered activated carbon. *J. Clean. Prod.* **2009**, *17*, 1223–1227. [[CrossRef](#)]
- Ghunmi, L.A.; Zeeman, G.; Fayyad, M.; van Lier, J.B. Grey water treatment systems: A review. *Crit. Rev. Environ. Sci. Technol.* **2011**, *41*, 657–698. [[CrossRef](#)]
- Li, F.; Wichmann, K.; Otterpohl, R. Review of the technological approaches for grey water treatment and reuses. *Sci. Total Environ.* **2009**, *407*, 3439–3449. [[CrossRef](#)] [[PubMed](#)]
- Fujishima, A.T.; Rao, N.; Tryk, D.A. Titanium dioxide photocatalysis. *J. Photochem. Photobiol. C* **2000**, *1*, 1–21. [[CrossRef](#)]
- Malato, S.; Fernández-Ibáñez, P.; Maldonado, M.I.; Blanco, J.; Gernjak, W. Decontamination and disinfection of water by solar photocatalysis: Recent overview and trends. *Catal. Today* **2009**, *147*, 1–59. [[CrossRef](#)]
- McGuigan, K.G.; Conroy, R.M.; Mosler, H.-J.; du Preez, M.; Ubomba-Jaswa, E.; Fernández-Ibáñez, P. Solar water disinfection (SODIS): A review from bench-top to roof-top. *J. Hazard. Mater.* **2012**, *235–236*, 29–46. [[CrossRef](#)] [[PubMed](#)]
- Egerton, T.A. The Influence of surface alumina and silica on the photocatalytic degradation of organic pollutants. *Catalysts* **2013**, *3*, 338–362. [[CrossRef](#)]
- Nakano, R.; Hara, M.; Ishiguro, H.; Yao, Y.; Ochiai, T.; Nakata, K.; Murakami Kajioka, J.; Sunada, K.; Hashimoto, K.; Fujishima, A.; *et al.* Broad spectrum microbicidal activity of photocatalysis by TiO₂. *Catalysts* **2013**, *3*, 310–323. [[CrossRef](#)]
- Park, J.; Kettleison, E.; An, W.-J.; Tang, Y.J.; Biswas, P. Inactivation of *E. coli* in water using photocatalytic, nanostructured films synthesized by aerosol routes. *Catalysts* **2013**, *3*, 247–260. [[CrossRef](#)]
- Vijay, M.; Ramachandran, K.; Ananthapadmanabhan, P.V.; Nalini, B.; Pillai, B.C.; Bondioli, F.; Manivannan, A.; Narendhirakannan, R.T. Photocatalytic inactivation of Gram-positive and Gram-negative bacteria by reactive plasma processed nanocrystalline TiO₂ powder. *Curr. Appl. Phys.* **2013**, *13*, 510–516. [[CrossRef](#)]
- Marugán, J.; van Grieken, R.; Pablos, C.; Satuf, M.L.; Cassano, A.E.; Alfano, O.M. Photocatalytic inactivation of *Escherichia coli* aqueous suspensions in a fixed-bed reactor. *Catal. Today* **2015**, *252*, 143–149. [[CrossRef](#)]

16. Adán, C.; Marugán, J.; Mesones, S.; Casado, C.; van Grieken, R. Bacterial inactivation and degradation of organic molecules by titanium dioxide supported on porous stainless steel photocatalytic membranes. *Chem. Eng. J.* **2016**, in press.
17. Lazar, M.A.; Varghese, S.; Nair, S.S. Photocatalytic water treatment by titanium dioxide: Recent updates. *Catalysts* **2012**, *2*, 572–601. [[CrossRef](#)]
18. Ibhaddon, A.O.; Fitzpatrick, P. Heterogeneous Photocatalysis: Recent Advances and Applications. *Catalysts* **2013**, *3*, 189–218. [[CrossRef](#)]
19. Gulyas, H.; Argáez, A.S.O.; Kong, F.; Liriano Jorge, C.; Eggers, S.; Otterpohl, R. Combining activated carbon adsorption with heterogeneous photocatalytic oxidation: Lack of synergy for biologically treated greywater and tetraethylene glycol dimethyl ether. *Environ. Technol.* **2013**, *34*, 1393–1403. [[CrossRef](#)] [[PubMed](#)]
20. Zhu, X.; Nanny, M.A.; Butler, E.C. Photocatalytic oxidation of aqueous ammonia in model gray waters. *Water Res.* **2008**, *42*, 2736–2744. [[CrossRef](#)] [[PubMed](#)]
21. Sanchez, M.; Rivero, M.J.; Ortiz, I. Photocatalytic oxidation of grey water over titanium dioxide suspensions. *Desalination* **2010**, *262*, 141–146. [[CrossRef](#)]
22. Gulyas, H.; Jain, H.B.; Susanto, A.L.; Malekpur, M.; Harasiuk, K.; Krawczyk, I.; Choromanski, P.; Furmanska, M. Solar photocatalytic oxidation of Pretreated wastewaters: Laboratory scale generation of design data for technical-scale double-skin sheet reactors. *Environ. Technol.* **2004**, *26*, 501–514. [[CrossRef](#)] [[PubMed](#)]
23. Von Wandruszka, R. Humic acids: Their detergent qualities and potential uses in pollution remediation. *Geochem. Trans.* **2000**, *1*, 10–15. [[CrossRef](#)]
24. Edzwald, J.K.; Becker, W.C.; Wattier, K.L. Surrogate parameters for monitoring organic matter and THM precursors. *J. AWWA* **1985**, *77*, 122–132.
25. Uyguner, C.S.; Bekbolet, M. Evaluation of humic acid photocatalytic degradation by UV-vis and fluorescence spectroscopy. *Catal. Today* **2005**, *101*, 267–274. [[CrossRef](#)]
26. Huang, X.; Leal, M.; Li, Q. Degradation of natural organic matter by TiO₂ photocatalytic oxidation and its effect on fouling low-pressure membranes. *Water Res.* **2008**, *42*, 1142–1150. [[CrossRef](#)] [[PubMed](#)]
27. Jin-hui, Z. Research on UV/TiO₂ photocatalytic oxidation of organic matter in drinking water and its influencing factors. *Procedia Environ. Sci.* **2012**, *12*, 445–452. [[CrossRef](#)]
28. Pablos, C.; van Grieken, R.; Marugán, J.; Moreno, B. Photocatalytic inactivation of bacteria in a fixed-bed reactor: Mechanistic insights by epifluorescence microscopy. *Catal. Today* **2011**, *161*, 133–139. [[CrossRef](#)]
29. Faure, M.; Gerardin, F.; André, J.-C.; Pons, M.-N.; Zahraa, O. Study of photocatalytic damages induced on *E. coli* by different photocatalytic supports (various types and TiO₂ configurations). *J. Photochem. Photobiol.* **2011**, *222*, 323–329. [[CrossRef](#)]
30. Bekbolet, M.; Araz, C.V. Inactivation of *Escherichia coli* by photocatalytic oxidation. *Chemosphere* **1996**, *32*, 959–965. [[CrossRef](#)]
31. Bekbolet, M. Photocatalytic bactericidal activity of TiO₂ in aqueous suspensions of *E. coli*. *Water Sci. Technol.* **1997**, *35*, 95–100. [[CrossRef](#)]
32. Bekbolet, M. Photocatalytic Inactivation of Microorganisms in Drinking Water. In *Control of Disinfection By-Products in Drinking Water Systems*; Nikolau, A., Selcuk, H., Rizzo, L., Eds.; NOVA Science Publishers: New York, NY, USA, 2007; pp. 97–117.
33. Chen, Y.; Lu, A.; Li, Y.; Yip, H.Y.; An, T.; Li, G.; Jin, P.; Wang, P.-K. Photocatalytic inactivation of *Escherichia coli* by natural sphalarite suspension: Effect of spectrum, wavelength and intensity of visible light. *Chemosphere* **2011**, *84*, 1276–1281. [[CrossRef](#)] [[PubMed](#)]
34. Marugán, J.; van Grieken, R.; Pablos, C.; Sordo, C. Analogies and differences between photocatalytic oxidation of chemicals and photocatalytic inactivation of microorganisms. *Water Res.* **2010**, *44*, 789–796. [[CrossRef](#)] [[PubMed](#)]
35. Pal, A.; Pehkonen, S.O.; Yu, L.E.; Ray, M.B.V. Photocatalytic inactivation of Gram-positive and Gram-negative bacteria using fluorescent light. *J. Photochem. Photobiol. A* **2007**, *186*, 335–341. [[CrossRef](#)]
36. Van Grieken, R.; Marugán, J.; Pablos, C.; Furones, L.; López, A. Comparison between the photocatalytic inactivation of Gram-positive *E. faecalis* and Gram-negative *E. coli* faecal contamination indicator microorganisms. *Appl. Catal. B* **2010**, *100*, 212–220. [[CrossRef](#)]

37. Buxton, G.V.; Greenstock, C.L.; Helman, W.P.; Ross, A.B. Critical review of rate constants for reactions of hydrated electrons, hydrogen atoms and hydroxyl radicals in aqueous solutions. *J. Phys. Chem. Ref. Data* **1988**, *175*, 13–886.
38. Uyguner, C.S.; Bekbolet, M. Application of photocatalysis for the removal of natural organic matter in simulated surface and ground waters. *J. Adv. Oxid. Technol.* **2009**, *12*, 87–92.
39. Uyguner-Demirel, C.S.; Birben, C.; Bekbolet, M. Key role of common anions on the photocatalytic degradation profiles of molecular size fractions of humic acids. *Catal. Today* **2013**, *209*, 122–126. [[CrossRef](#)]
40. Bekbolet, M.; Boyacioglu, Z.; Ozkaraova, B. The influence of solution matrix on the photocatalytic removal of color from natural waters. *Water Sci. Technol.* **1998**, *38*, 155–162. [[CrossRef](#)]
41. Abdullah, M.; Low, G.K.-W.; Matthews, R.W. Effects of common inorganic anions on rates of photocatalytic oxidation of organic carbon over illuminated titanium dioxide. *J. Phys. Chem.* **1990**, *94*, 6820–6825. [[CrossRef](#)]
42. Rincón, A.-G.; Pulgarin, C. Effect of pH, inorganic anions, organic matter and H₂O₂ on *E. coli* K12 photocatalytic inactivation by TiO₂: Implications in solar water disinfection. *Appl. Catal. B* **2004**, *51*, 283–302. [[CrossRef](#)]
43. Pulgarin, C.; Kiwi, J.; Nadtochenko, V. Mechanism of photocatalytic bacterial inactivation on TiO₂ films involving cell-wall damage and lysis. *Appl. Catal. B* **2012**, *128*, 179–183. [[CrossRef](#)]
44. Christl, I.; Kretzschmar, R. Relating ion binding by fulvic and humic acids to chemical composition and molecular size. Proton binding. *Environ. Sci. Technol.* **2001**, *35*, 2512–2517. [[CrossRef](#)] [[PubMed](#)]
45. Carp, O.; Huisman, C.L.; Reller, A. Photoinduced reactivity of titanium dioxide. *Solid State Phenom.* **2004**, *32*, 33–177. [[CrossRef](#)]
46. Bekbolet, M.; Suphandag, A.S.; Uyguner, C.S. An investigation of the photocatalytic efficiencies of TiO₂ powders on the decolourisation of humic acids. *J. Photochem. Photobiol. A* **2002**, *148*, 121–128. [[CrossRef](#)]
47. Christova-Boal, D.; Eden, R.E.; McFarlane, S. An investigation into greywater reuse for urban residential properties. *Desalination* **1996**, *106*, 391–397. [[CrossRef](#)]
48. Nolde, E. Grey water reuse systems for toilet flushing in multi-storey buildings-over ten years experience in Berlin. *Urban Water* **1999**, *1*, 275–284. [[CrossRef](#)]
49. Dixon, A.M.; Butler, D.; Fewkes, A. Guidelines for grey water reuse: Health issues. *J. CIWEM* **1999**, *13*, 322–326.
50. American Public Health Association; American Water Works Association; Water Environment Federation. *Standard Methods for the Examination of Water and Wastewater*, 22nd ed.; American Water Works Association: Washington, DC, USA, 2012.
51. Kerc, A.; Bekbolet, M.; Saatci, A.M. Effects of oxidative treatment techniques on molecular size distribution of humic acids. *Water Sci. Technol.* **2004**, *49*, 7–12.



© 2016 by the authors; licensee MDPI, Basel, Switzerland. This article is an open access article distributed under the terms and conditions of the Creative Commons Attribution (CC-BY) license (<http://creativecommons.org/licenses/by/4.0/>).